Supramolecular tuning of energy transfer efficiency and direction in a bis(styryl) dye–crown ether conjugate

Daria V Berdnikova, Yuri V Fedorov, lga A Fedorova, Gediminas Jonusauskas

Supramolecular tuning of energy transfer efficiency and direction in a bis(styryl) dye–crown ether conjugate

Daria V. Berdnikova[a,b,*,1], Yuri V. Fedorov[a], Olga A. Fedorova[a], Gediminas Jonusauskas[c]

[a] A. N. Nesmeyanov Institute of Organoelement Compounds, Russian Academy of Sciences, Vavilova str. 28, 119991 Moscow, Russia
[b] RUDN University, Mikluho-Maklaya str. 6, 117198 Moscow, Russia
[c] Laboratoire Ondes et Matière d'Aquitaine – UMR CNRS 5798, Bordeaux University, Talence 33405, France

ARTICLE INFO

Keywords:
Bis(styryl) dye
Energy transfer
FRET
Crown ether
Cation complexation
Protonation

ABSTRACT

The control of the energy transfer (FRET) in a novel bischromophoric styryl(pyridinium) dye bearing two different crown ether residues is presented. Complexation of the dye with metal cations allows to tune the FRET efficiency without changing the transfer direction or to switch the FRET off, whereas protonation launches the FRET process in the opposite direction relative to the molecular structure.

1. Introduction

Photoinduced resonance energy transfer (FRET) is one of the basic processes in Nature that ensures photosynthetic conversion of the solar energy into chemical bonds in living organisms [1]. In artificial systems, photoinduced energy transfer is widely used in solar energy harvesting elements, ratiometric sensors, and organic photovoltaics [2 6]. Most of these applications require a stringent control of the FRET rate, efficiency and, especially, the direction. Along these lines, it is highly desirable that the direction of the energy transfer can be switched on demand. For example, such switching has been realized by changing the complexed metal cations in homo and heterodimers of metalloporphyrins [7], metallocyclodextrin assemblies [8] and [2] catenates incorporating the $[Ru(tpy)_2]^{2+}$ fragment [9]. The control of the FRET direction can be also accomplished by protonation/deprotonation of the donor or acceptor unit as has been shown for oligophenylene vinylene (OPV) phenanthroline [10] and OPV fullerene [11] dyads and for multichromophoric BODIPY systems [12,13]. In addition, several intriguing examples of switchable FRET directions have been reported that use site specific solvent effects [14], temperature changes [15] or the electronic difference between cation binding sites [16,17]. Nevertheless, molecules or molecule assemblies that enable the fine regulation of the energy transfer processes based on supramolecular interactions are still rare and their discovery and development remains a topical challenge.

Herein, we present a dye crown ether conjugate whose energy transfer efficiency and direction is controlled by supramolecular complexation and protonation. The system is based on a novel bischromophoric styryl derivative **1** that is functionalized with benzo 15 crown 5 and azadithia 15 crown 5 ether units (Chart 1). Owing to the different affinity of the crown ether fragments towards metal ions or protons, the optical properties of each chromophore can be varied independently by introduction of appropriate metal cations or protonation, thus enabling the control of the energy transfer properties.

2. Results and discussion

2.1. Synthesis of bis(styryl) dye 1

The bis(styryl) dye **1** was obtained in 42% yield by condensation of the corresponding formylbenzocrown derivatives with γ picoline and subsequent quaternization of the intermediate styryl(pyridine) species with 1,4 bis(bromomethyl)benzene (for details see ESI, Section 1). The parent monochromophoric dyes **2** and **3** were synthesized according to published protocols [18,19].

2.2. Steady state optical spectroscopy

The absorption spectrum of bis(styryl) dye **1** exhibits two long wavelength absorption bands centered at 420 and 486 nm (Fig. 1, Table 1). Comparison with the absorption spectra of the related monochromophoric dyes **2** (λ_{abs} = 395 nm) [18] and **3** (λ_{abs} = 474 nm)

* Corresponding author. A. N. Nesmeyanov Institute of Organoelement Compounds, Russian Academy of Sciences, Vavilova str. 28, 119991 Moscow, Russia.
E-mail addresses: berdnikova@chemie-bio.uni-siegen.de, daria@ineos.ac.ru (D.V. Berdnikova).
[1] Present address: Universität Siegen, Organische Chemie II, Adolf-Reichwein-Str. 2, 57068 Siegen, Germany.

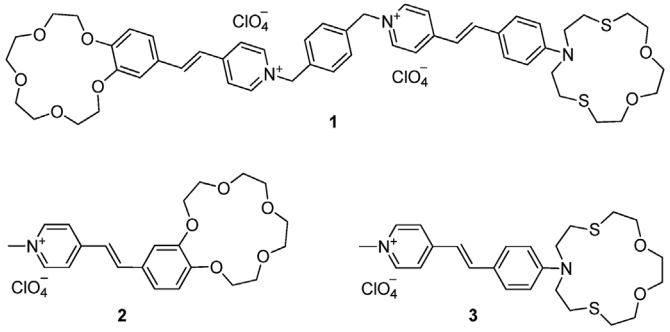

Chart 1. Chemical structures of styryl dyes **1**–**3**.

[19] in acetonitrile, respectively (Figs. S3 and S4, ESI), allowed to assign the band at 420 nm to the benzocrown substituted styryl chromophore of dye **1** and the band at 486 nm to the azadithiacrown substituted one. For the sake of clarity, the benzocrown functionalized chromophore will be referred to as the O chromophore and the azadithiacrown functionalized one as the N chromophore, to indicate that the respective electron donating heteroatom of the crown ether, that is directly conjugated with the styryl(pyridinium) fragment, determines the photophysical properties of the chromophore.

Complexation of the crown ether functionalities of dye **1** with metal cations leads to a blue shift of the corresponding absorption bands. It is known that oxacrown ethers have a high affinity to alkali and alkali earth metal ions [20], whereas the introduction of N or/and S atoms leads to higher affinity towards transition metal ions [21]. Based on this difference, the attachment of different crown ethers with diverse heteroatom substitution to the two chromophoric parts of **1** enables the independent regulation of the optical properties of each chromophore by complexation with appropriate cations. For the present study, we have selected Mg^{2+} and Hg^{2+} cations as they have the most effective interaction with the corresponding crown ethers [22,23]. The metal cations were used as perchlorate salts. To avoid introduction of different anions that may potentially influence complexation, we used perchloric acid for protonation of the azadithiacrown ether residue.

Addition of $Mg(ClO_4)_2$ to a solution of **1** results in a blue shift ($\Delta\lambda = 52$ nm) of the O chromophore absorption whereas the N chromophore absorption remains unaffected (Fig. 1A, Table 1). Conversely, the introduction of $Hg(ClO_4)_2$ and $HClO_4$ causes a blue shift of the N chromophore absorption ($Hg(ClO_4)_2$: $\Delta\lambda = 124$ nm; $HClO_4$: $\Delta\lambda = 148$ nm) without significant changes of the O chromophore absorption (Fig. 1B and C, Table 1). The stability constants of the complexes of **1** were obtained from the spectrophotometric titration data (Figs. S1 and S2, ESI) and are collected in Table 1.

According to the classical description of the Förster resonance energy transfer (FRET), an efficient energy transfer requires a spectral overlap between the emission of the donor and the absorption of the acceptor chromophores [24,25]. To estimate the potential for an intramolecular energy transfer in dye **1** and its complexes, the optical characteristics of each chromophore were assessed separately with parent monochromophoric dyes **2** and **3** and their complexes with Mg^{2+}, Hg^{2+} and H^+. The fluorescence of **2** overlaps significantly with the absorption of **3** (Fig. 2A). Therefore, within the bischromophoric dye **1**, the O chromophore may act as an energy donor (ED), whereas the N chromophore is an energy acceptor (EA). The blue shift of the fluorescence of **2** upon complexation with Mg^{2+} provides more pronounced spectral overlap between the fluorescence of the O chromophore (ED) and the absorption of the N chromophore (EA) (Fig. 2B), thus favoring energy transfer in complex **1** Mg^{2+}. At the same time, the absorption and fluorescence spectra of dye **2** and complex **3** Hg^{2+} do not overlap so that an energy transfer is not feasible in the complex of dye **1** with Hg^{2+} (Fig. S5, ESI). Protonation of dye **3** results in a sufficient spectral overlap of the fluorescence of **3** H^+ and the absorption of **2** which leads to a reversal of the donor and acceptor functions of the chromophores in the energy transfer process (Fig. 2C). Thus, in the bischromophoric system **1** H^+ the protonated N chromophore acts as energy donor and the O chromophore as energy acceptor.

Table 1
Optical properties and stability constants of **1** and its complexes in acetonitrile.

Compound	λ_{abs}, nm	$\varepsilon \times 10^{-4}$, L mol^{-1} cm^{-1}	log *K*
1	420, 486	3.27, 3.63	–
1-Mg^{2+}	368, 486	3.12, 3.71	3.27 ± 0.03
1-Hg^{2+}	373, 393	3.37, 3.43	> 7[a]
1-H^+	404, 338	3.96, 3.07	3.38 ± 0.01

[a] The value is too high to be determined from spectrophotometric titration.

2.3. Theoretical calculation of the energy transfer efficiency

To estimate the efficiency of the energy transfer in **1** and its complexes **1** Mg^{2+} and **1** H^+, we performed calculations according to Förster resonance theory (for details seeESI, Section 5) [25]. Taking into account the crucial influence of the interchromophoric distance on FRET efficiency, on one side, and high conformational lability of **1**, on the other side, we considered two extreme conformations of dye **1** with maximally close and maximally remote mutual positions of the chromophores (Fig. S11, ESI). After geometry optimization (MOPAC 2016, PM7), the corresponding interchromophoric distances were determined as $r_{max} = 15$ Å and $r_{min} = 9$ Å. Based on these values, we obtained the following theoretical intervals of the FRET efficiencies Φ_{FRET} (th): 97.4 99.9% for **1**, 93.7 99.7% for **1** Mg^{2+} and 42.8 94.1% for **1** H^+. Therefore, the expected FRET efficiencies in the studied species in most cases are very high. At the same time, the pronounced difference in the theoretical values Φ_{FRET} (th) for two extreme conformations of complex **1** H^+ arises from the relatively small value of the Förster radius $R_0 = 14$ Å, i.e. the distance at which the energy transfer efficiency is

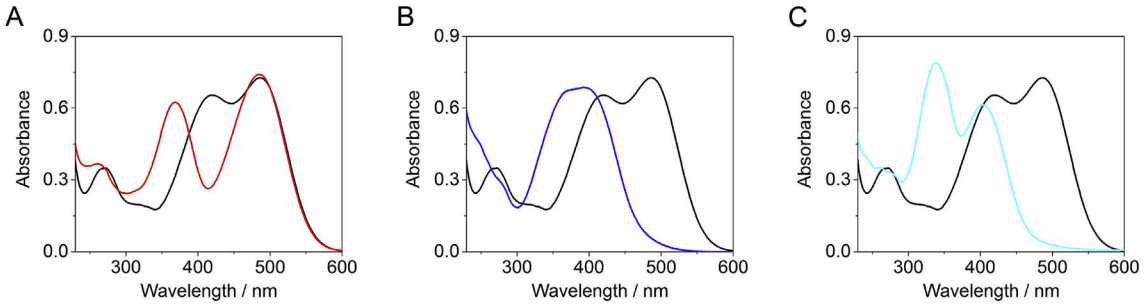

Fig. 1. Absorption spectra of **1** (black), (A) complex **1**-Mg^{2+} (red) with the Mg^{2+} cation bound to the benzocrown ether residue; (B) complex **1**-Hg^{2+} (blue) with the Hg^{2+} cation bound to the azadithia-crown ether residue; (C) protonated form **1**-H^+ (cyan) with a proton bound to the crown ether nitrogen. In all cases $c = 20$ μM, in acetonitrile, $T = 20$ °C. (For interpretation of the references to colour in this figure legend, the reader is referred to the Web version of this article.)

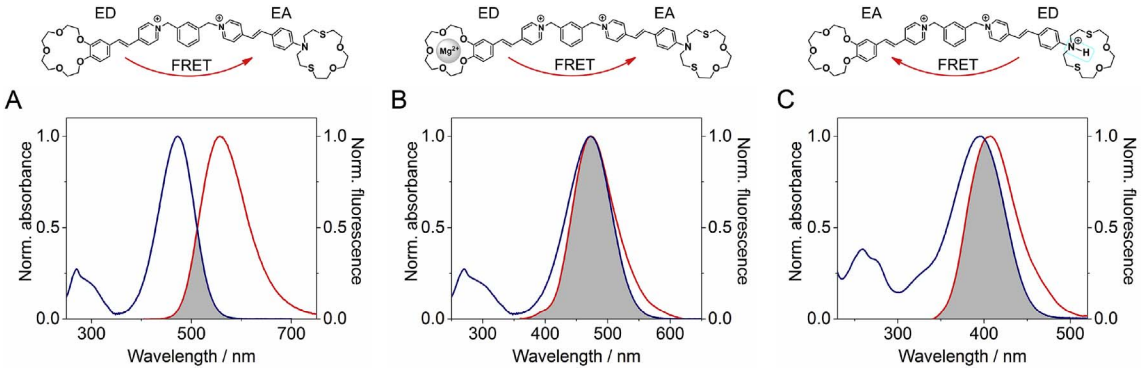

Fig. 2. Spectral overlap (grey area) between (A) the normalized fluorescence spectrum of **2** (red, ED) and normalized absorption spectrum of **3** (blue, EA); (B) the normalized fluorescence spectrum of **2**-Mg^{2+} (red, ED) and normalized absorption spectrum of **3** (blue, EA); (C) the normalized fluorescence spectrum of **3**-H^+ (red, ED) and normalized absorption spectrum of **2** (blue, EA) in acetonitrile. (For interpretation of the references to colour in this figure legend, the reader is referred to the Web version of this article.)

50% [25], for this complex in comparison to **1** and complex **1** Mg^{2+} (Table S1, ESI). For **1** H^+, r_{max} = 15 Å that is larger than R_0 which leads to the drastic decrease of the estimated FRET efficiency for the corre sponding conformation.

2.4. Time resolved fluorescence spectroscopy

The emission properties of **1** and its complexes **1** Mg^{2+} and **1** H^+ were studied by steady state and time resolved fluorescence spectro scopy. Upon excitation of dye **1** in the O chromophore absorption band, emission of both chromophores was detected in the steady state and time resolved fluorescence spectra (Fig. 3A; Fig. S6, ESI). This result indicates that for a part of the excited molecules, energy transfer from the O chromophore to the N chromophore does not occur.

Since two different excited states are formed upon photoexcitation of dye **1**, its relaxation should follow two main pathways. Thus, for a part of the molecules the excited state relaxation occurs through emission of the N chromophore that is either excited directly or in directly by energy transfer from the excited O chromophore. For the remaining molecules with the excited O chromophore, energy transfer does not occur and the system relaxes according to the deactivating pathways of the O chromophore. The resulting fluorescence lifetimes support this assumption (Fig. 4A). The fast component of the decay kinetics belongs to the relaxation of the N chromophore through the formation of TICT states due to the rotation around the single bond in the CH PhN fragment [26], as supported by close τ_1 values for dye **1** and parent monochromophoric dye **3** (Table 2). The slow component of the kinetics represents an averaged value of both decay times of the O chromophore as compared with the τ values of the parent mono chromophoric dye **2** (Table 2).

Due to the significant blue shift of the Mg^{2+} bound O chromophore absorption (ED), the donor can be excited selectively at 350 nm because the N chromophore (EA) has almost no absorption at this wavelength (Fig. S4, ESI). As can be seen from the steady state and time resolved fluorescence spectra (Fig. 3B; Fig. S7, ESI), the excitation of the com plex **1** Mg^{2+} at 350 nm leads only to one fluorescence band centered at 620 nm that corresponds to the emission of the N chromophore (EA), which indicates the occurrence of an efficient energy transfer from the Mg^{2+} complexed O chromophore (ED) to the N chromophore (EA). Accordingly, the fast component of the decay kinetics of **1** Mg^{2+} is assigned to the emission of the N chromophore (EA) through TICT states as in the parent dye **3** (Fig. 4B, Table 2). The residual long lived second component belongs to the trace amount of non complexed O chromophore due to relatively low stability constant of complex **1** Mg^{2+}.

In the case of protonated dye **1** H^+ the donor and acceptor functions of the chromophores are reversed in the energy transfer process, namely, the protonated N chromophore acts as ED and the O chromo phore becomes EA. Accordingly, excitation of complex **1** H^+ at 350 nm results in only one fluorescence band in the region of 560 nm that be longs to the emission of O chromophore (EA) (Fig. 3C; Fig. S8, ESI). The fluorescence decay curve of **1**-H^+ is biexponential (Fig. 4C) which is typical for the relaxation of the O chromophore (*cf.* τ values for com pound **2**, Table 2). The fast component is assigned to the relaxation through TICT states, whereas the slow component corresponds to the *E Z* isomerization [27].

To obtain the experimental values of the FRET efficiencies, the rate of the energy transfer process in **1** and its complexes **1** Mg^{2+} and **1** H^+ was determined with ultrafast transient absorption spectroscopy (TRABS). Representative results from TRABS experiments in the case of energy transfer towards the N chromophore (free **1**, complex **1** Mg^{2+}) are displayed in Fig. 5A taking **1** Mg^{2+} as example. There are three main processes occurring after the pump pulse: i) absorption of the dimethylaniline cation radical at about 450 nm [28], ii) ground state bleaching of the N chromophore at the region of 500 nm, and iii) sti mulated emission of the N chromophore at about 620 nm (Fig. 5A; Fig. S9, ESI). The time dependent red shift of the stimulated emission maximum arises from the dynamic solvent relaxation that reflects the rearrangement of the solvent molecules around the excited chromo phore, whose polarity changes in comparison to the ground state due to the photoinduced intramolecular charge transfer (ICT). In the case of energy transfer towards the O chromophore (protonated dye **1** H^+),

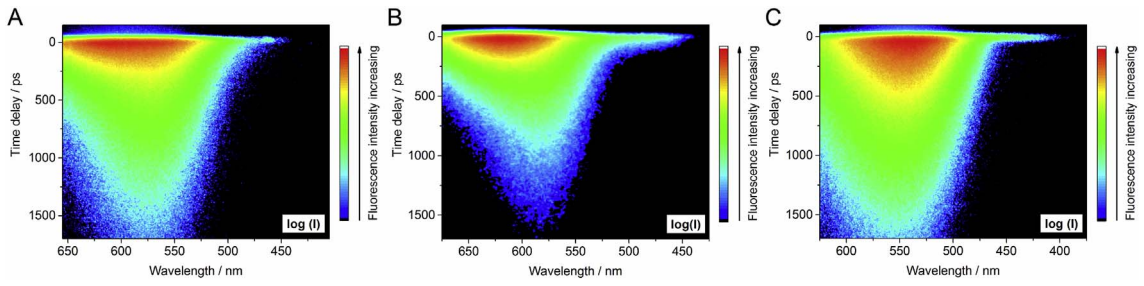

Fig. 3. Time-resolved fluorescence maps of (A) **1**, λ_{ex} = 400 nm, (B) **1**-Mg^{2+}, λ_{ex} = 350 nm, and (C) **1**-H^+, λ_{ex} = 350 nm, in acetonitrile.

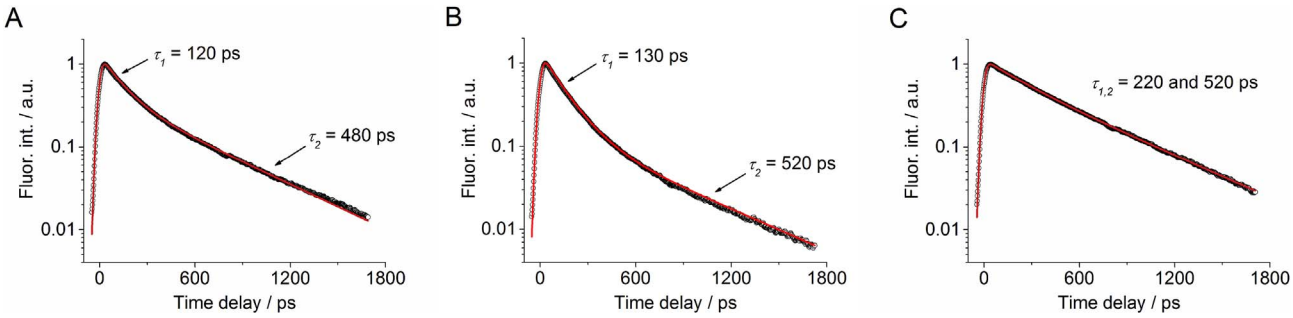

Fig. 4. Fluorescence decay curves in acetonitrile: (A) **1**, λ_{ex} = 400 nm, λ_{obs} = 580 nm; (B) **1**-Mg^{2+}, λ_{ex} = 350 nm, λ_{obs} = 620 nm; and (C) **1**-H^{+}, λ_{ex} = 350 nm, λ_{obs} = 550 nm; experimental data: empty circles, fitting curve: red line. (For interpretation of the references to colour in this figure legend, the reader is referred to the Web version of this article.)

Table 2
Fluorescence lifetimes τ, energy transfer time constants τ_{FRET}, theoretical Φ_{FRET} (th) and experimental Φ_{FRET} (exp) energy transfer efficiencies for dye **1**, its complexes **1**-Mg^{2+} and **1**-H^{+} in acetonitrile. Fluorescence lifetimes τ for dyes **2** and **3** in acetonitrile.

Compound	τ, ps	τ_{FRET}, ps	Φ_{FRET} (th), %	Φ_{FRET} (exp), %
1	120, 480	0.150	97.4–99.9	100.0
1-Mg^{2+}	130, 520	0.150	93.7–99.7	99.8
1-H^{+}	220, 520	0.220	42.8–94.1	95.6
2	310, 650[a]	–	–	–
3	100, 230[b]	–	–	–

[a] Data from Ref. [27].
[b] Data from Ref. [19].

two processes are observed on a TRABS map, namely: i) absorption of the isomeric dimethoxybenzene cation radicals at 450 nm [29] and ii) stimulated emission of the O chromophore at the region of 550 nm (Fig. 5B).

Analysis of the TRABS data allowed to determine the energy transfer time constants τ_{FRET} (Table 2; Fig. S10, ESI). For free dye **1** and its complex **1** Mg^{2+}, τ_{FRET} data were obtained from the ground state bleaching kinetics of the energy acceptor (N chromophore) at 500 nm and 505 nm, respectively (Figs. S10A and S10B, ESI). For the protonated form **1** H^{+}, τ_{FRET} was determined from the kinetics of development of the stimulated emission band of the energy acceptor (O chromophore) at 525 nm (Fig. S10C, ESI). Experimental energy transfer efficiencies Φ_{FRET} (exp) were calculated from the τ_{FRET} values according to Equation (1).

$$\Phi_{FRET} = (1 - \tau_{FRET}/\tau_0)\cdot 100\% \quad (1)$$

In equation (1), τ_{FRET} is energy transfer time constant obtained from the TRABS experiment, τ_0 is excited state lifetime of the energy donor in the absence of the energy acceptor.

In free dye **1**, the energy donor is the O chromophore, whose excited state lifetime of τ_0 = 650 ps was determined from the fluorescence decay kinetics of dye **2** that contains the isolated O chromophore [27].

In the case of complex **1** Mg^{2+}, we considered the reported lifetime of τ_0 = 70 ps of the magnesium complex of dye **2** [27]. For the protonated form **1** H^{+}, in which the energy donor is the protonated N chromophore, the lifetime of τ_0 ~ 5 ps was estimated tentatively from the fluorescence decay kinetics of the protonated dye **3** H^{+} that contains the isolated N chromophore [19]. As can be seen from Table 2, the experimental FRET efficiencies Φ_{FRET} (exp) in the studied systems are very high and in the case of free dye **1** and the complex **1** Mg^{2+} exceed 99%.

Based on the previous discussion, the reasons for the incomplete energy transfer in dye **1** still need to be explained. As was shown, the evaluation of both theoretical and experimental data revealed a > 99% FRET efficiency for **1**. At the same time, clear presence of the fluorescence of energy donor (O chromophore) at the region of 560 nm (Fig. 3A; Fig. S6, ESI) indicates that some of the excited molecules of **1** are not involved in the FRET process. Since the relative orientation of the dipole transition moments of the ED and the EA significantly influences the efficiency of the FRET [24], we assume that energy transfer in **1** cannot be realized partially for geometrical reasons. In theoretical calculations, we considered the random orientation of the chromophores in **1** due to the high conformational flexibility of the xylylene spacer (for details see ESI, Section 6). This flexibility, however, is true only for the isolated molecules of **1** in solution. At the same time, it is known that charged styryl dyes readily undergo dipole dipole aggregation due to the highly polar character of the chromophores [30]. Considering the significantly restricted freedom of movement of the aggregated molecules, it is tempting to assume that the aggregation locks some dye molecules in a geometry that is unfavorable for energy transfer.

To provide evidence for the aggregation, we analyzed the absorption spectra of dye **1** and an equimolar mixture of the parent dyes **2** and **3** (Fig. 6). Hence, deconvolution of the spectrum of the monomeric dyes mixture with Gaussian shaped absorption bands gave two components at about 21000 and 25000 cm^{-1} corresponding to the absorption spectra of the individual chromophores (Fig. 6A). Deconvolution of the

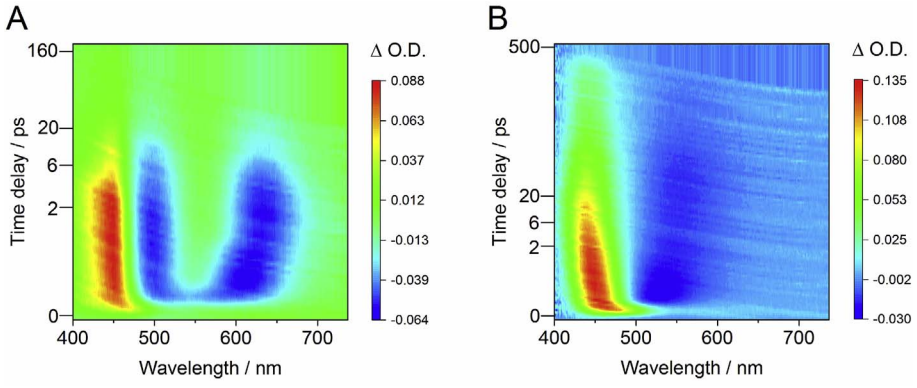

Fig. 5. Time-resolved TRABS maps for (A) **1**-Mg^{2+} and (B) **1**-H^{+}, λ_{ex} = 345 nm, acetonitrile.

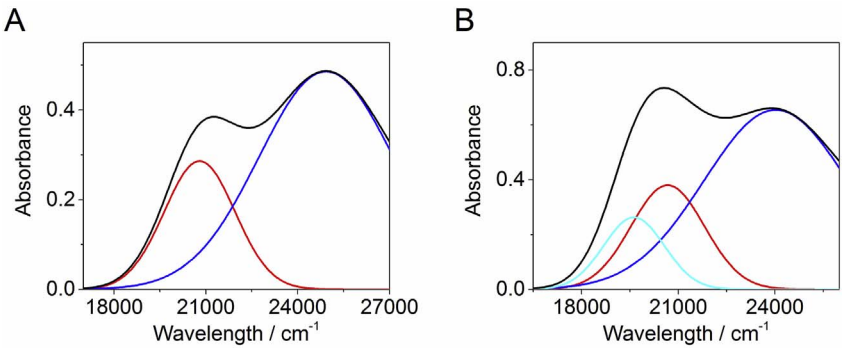

Fig. 6. (A) Absorption spectrum of the equimolar mixture of monomeric dyes **2** and **3** (black, for each dye $c = 20\,\mu M$) and its deconvolution: blue line corresponds to the O-chromophore, red line corresponds to the N-chromophore. (B) Absorption spectrum of bischromophoric dye **1** (black, $c = 20\,\mu M$) and its deconvolution: blue line corresponds to the O-chromophore, red line corresponds to the N-chromophore, and cyan line represents the absorption of the aggregates. (For interpretation of the references to colour in this figure legend, the reader is referred to the Web version of this article.)

spectrum of bischromophoric dye **1** showed the presence of the same bands as in the case of the monomeric dyes mixture and additionally revealed the third component at about 19500 cm^{-1} (Fig. 6B). This new band is shifted to the lower energy region that is indicative of the formation of J type aggregates [31]. The detailed investigation of the aggregation pattern, however, falls beyond the scope of the present manuscript.

As a result, the spectral analysis supports the aggregation of **1** that is proposed to be a likely reason for incomplete energy transfer due to geometrical reasons. At the same time, for non aggregated molecules of **1** the efficiency of FRET is close to 100% as indicated by experimentally obtained energy transfer efficiencies Φ_{FRET} (exp) and additionally supported by the theoretical calculations (Table 2). Unlike dye **1**, the complexes **1** Mg^{2+} and **1** H^+ show no fluorescence of the ED (Fig. 3B and C) which is in agreement with both theoretical and experimental Φ_{FRET} values (Table 2). We explain this observation by dissociation of the aggregates upon complexation due to the decrease of the dipole moments of complexed chromophores and the increase of the overall positive charge of the molecules resulting in the electrostatic repulsion between aggregated molecules.

3. Conclusions

To sum up, we have designed and synthesized the novel bis(styryl) dye **1** bearing benzo 15 crown 5 and azadithia 15 crown 5 functionalities. In the free state, dye **1** undergoes efficient intramolecular energy transfer whereas upon aggregation of **1** the FRET process is partially blocked. Complexation of Mg^{2+}, Hg^{2+} cations and protonation allow independent manipulation of the optical properties of each chromophore within a single dye molecule, thus enabling the regulation of the FRET parameters in **1** by supramolecular complexation. Interestingly, binding of **1** with Hg^{2+} cations results in drastic decrease of the FRET efficiency, whereas interaction with Mg^{2+} and H^+ has just slight influence on this parameter. Notably, complexation with Mg^{2+} does not change the energy transfer direction in comparison to free dye **1**, whereas protonation results in the reversion of the direction of FRET relative to the molecular structure.

4. Experimental section

All reagents and solvents were obtained from commercial sources and used as received. ^1H NMR spectra were recorded at 300 or 600 MHz, ^{13}C NMR spectra were recorded at 150 MHz at ambient temperature using 5 mm tubes. Chemical shifts were determined with accuracy of 0.01 ppm and 0.1 ppm for ^1H and ^{13}C spectra, respectively, and are given relative to the residual signal of the solvent that was used as internal reference. Spin spin coupling constants for the proton spectra were determined with accuracy of 0.2 Hz. The proton NMR signal assignments were performed using COSY and NOESY 2D NMR techniques. The carbon NMR signal assignments were performed by means of HSQC and HMBC 2D NMR techniques. Electrospray ionization (ESI) mass spectra were detected in the mode of full mass scanning of positive ions on a tandem dynamic mass spectrometer equipped with a mass analyzer with an octapole ionic trap. High resolution mass spectra were recorded on a time of flight instrument in a positive ion mode using electrospray ionization method. Elemental analysis was performed at the Laboratory of Microanalysis of A. N. Nesmeyanov Institute of Organoelement Compounds of RAS, Moscow, Russia. Electronic absorption spectra were measured on Varian Cary 100 spectrophotometer. Fluorescence spectra were recorded on a Fluorolog 3 spectrofluorometer. All measurements were carried out in conventional quartz cells of 10 mm pathlength at 20 °C. Preparation and handling of the solutions were carried out under red light.

Time resolved optical experiments were based on a femtosecond 1 kHz Ti:Sapphire system producing 30 fs, 0.8 mJ laser pulses centered at 800 nm (Femtopower Compact Pro) coupled with an optical parametric generator (Light Conversion Topas C) and frequency mixers to excite samples at the maximum of the steady state absorption band. In the case of the time resolved fluorescence measurements, the fluorescence emitted by a sample in the forward direction was collected by reflective optics and focused with a spherical mirror onto the input slit of a spectrograph (Chromex 250) coupled to a streak camera (Hamamatsu 5680) equipped with a fast single sweep unit M5676, temporal resolution 2 ps. The convolution of a rectangular streak camera slit in the sweep range of 250 ps with an electronic jitter of the streak camera trigger pulse provided a Gaussian (over 4 decades) temporal apparatus function with a FWHM of 20 ps (for more details see ESI, Section 4.1). For the TRABS experiments, white light continuum (360 nm 1000 nm) pulses generated in a 2 mm D_2O cell were used as the probe. The variable delay time between excitation and probe pulses was obtained using a delay line with 0.66 fs resolution. The solutions were placed in a 2 mm circulating cell. White light signal and reference spectra were recorded using a two channel fibre spectrometer (Avantes Avaspec 2048 2). A home written acquisition and experiment control program in LabVIEW made it possible to record transient spectra with an average error less than 10^{-3} of optical density for all wavelengths. The temporal resolution of the set up was better than 50 fs (for more details see ESI, Section 4.2).

Note

Authors declare no competing financial interests.

Acknowledgements

This work was supported by RFBR (project 15 03 04705) and the Russian Science Foundation (project 16 13 10226). The publication was financially supported by the Ministry of Education and Science of the Russian Federation (the Agreement number 02.a03.0008). We thank Prof. Dr. Heiko Ihmels (Universität Siegen, Germany) for his kind assistance with the preparation of the manuscript.

[1] Hader DP, Tevini M. General photobiology. Oxford: Pergamon; 1987.
[2] Kundu S, Patra A. Chem Rev 2017;117:712.
[3] Fan J, Hu M, Zhan P, Peng X. Chem Soc Rev 2013;42:29.
[4] Hedley GJ, Ruseckas A, Samuel IDW. Chem Rev 2017;117:796.
[5] Hildebrandt N, Spillmann CM, Russ Algar W, Pons T, Stewart MH, Oh E, et al. Chem Rev 2017;117:536.
[6] Rowland CE, Delehanty JB, Dwyer CL, Medintz IL. Mater Today 2017;20:131.
[7] Sato S, Murakoshi K, Ikeda K. Chem Lett 2016;45:125.
[8] Haider JM, Williams RM, De Cola L, Pikramenou Z. Angew Chem Int Ed 2003;42:1830.
[9] Cárdenas DJ, Collin J-P, Gaviña P, Sauvage J-P, De Cian A, Fischer J, et al. J Am Chem Soc 1999;121:5481.
[10] Armaroli N, Eckert J-F, Nierengarten J-F. Chem Commun 2000:2105.
[11] Armaroli N, Accorsia G, Rioa Y, Nierengarten J-F, Eckert J-F, Gómez-Escalonilla MJ, et al. Synth Metals 2004;147:19.
[12] Puntoriero F, Nastasi F, Campagna S, Bura T, Ziessel R. Chem Eur J 2010;16:8832.
[13] Erbas-Cakmak S, Bozdemir OA, Cakmak Y, Akkaya EU. Chem Sci 2013;4:858.
[14] Indelli MT, Ghirotti M, Prodi A, Chiorboli C, Scandola F, McClenaghan ND, et al. Inorg Chem 2003;42:5489.
[15] Serroni S, Campagna S, Pistone Nascone R, Hanan GS, Davidson GJE, Lehn J-M.
[16] Ward MD, Barigelletti F. Coord Chem Rev 2001;216–217:127.
[17] Denti G, Serroni S, Campagna S, Ricevuto V, Balzani V. Coord Chem Rev 1991;111:227.
[18] Tulyakova EV, Fedorova OA, Fedorov Yu V, Jonusauskas G, Anisimov AV. Russ. Chem. Bull. Int. Ed 2007;56:2166..
[19] Tulyakova EV, Fedorova OA, Fedorov YV, Jonusauskas G, Anisimov AV. J Phys Org Chem 2008;21:372.
[20] Izatt RM, Terry RE, Nelson DP, Chan Y, Eatough DJ, Bradshaw JS, et al. J Am Chem Soc 1976;98:7626.
[21] For example, see Aragoni MC, Arca M, Bencini A, Blake AJ, Caltagirone C, Decortes A, et al. Dalton Trans 2005:2994.
[22] Tulyakova E, Delbaere S, Fedorov Y, Jonusauskas G, Moiseeva A, Fedorova O. Chem Eur J 2011;17:10752.
[23] Berdnikova DV, Fedorov YV, Fedorova OA. Dyes Pigments 2013;96:287.
[24] Van Der Meer BW, Coker G, Chen SYS. Resonance energy transfer: theory and data. New York: VCH; 1994.
[25] Lakowicz JR. Principles of fluorescent spectroscopy. New York: Springer science + Business Media, LLC, Plenum Publishers; 2006.
[26] (a) Grabowski ZR, Rotkiewicz K, Rettig W. Chem Rev 2003;103:3899;
(b) Strehmel B, Seifert H, Rettig W. J Phys Chem B 1997;101:2232.
[27] Marmois E. Étude photophysique de nouveaux systemes moleculaires fonctionnels bases sur les styrylpyridines L'Universite Bordeaux 1; 2008. Ph.D. dissertation.
[28] Shida T, Nosaka Y, Kato T. J Phys Chem 1978;82:695.
[29] O'Neill P, Steenken S, Schulte-Frohlinde D. J Phys Chem 1975;79:2773.
[30] (a) Behera GB, Behera PK, Mishra BK. J Surface Sci Technol 2007;23:1;
(b) Deligeorgiev T, Vasilev A, Kaloyanova S, Vaquero JJ. Color Technol 2010;126:55.
[31] (a) McRae EG, Kasha M. Augenstein L, Mason R, Rosenberg B, editors. Physical processes in radiation biology. New York: Academic; 1964. p. 23–42;
(b) Scherer POJ. Kobayashi T, editor. J-Aggregates. Singapore: World Scientific; 1996. p. 95–110.